

1 Article

## 2 Experimental Study on Drilling MDF with Tools 3 Coated with TiAlN and ZrN

4 Krzysztof Szwejka <sup>1,\*</sup>, Joanna Zielińska-Szwejka <sup>1</sup> and Tomasz Trzepieciniski <sup>2</sup>

5 <sup>1</sup> Faculty of Mechanical Engineering and Technology, Rzeszow University of Technology,  
6 Kwiatkowskiego 4, 37-450 Stalowa Wola, Poland; kszwejka@prz.edu.pl

7 <sup>2</sup> Department of Materials Forming and Processing, Rzeszow University of Technology,  
8 Powstancow Warszawy 8, 35-959 Rzeszow, Poland; tomtrz@prz.edu.pl

9 \* Krzysztof Szwejka: kszwejka@prz.edu.pl; Tel.: +48-695-695-456

10

11 **Abstract:** There is increasing use of wood-based composites in industry not only because of the  
12 shortage of solid wood, but above all for their better properties such as: strength, aesthetic  
13 appearance, etc. compared to wood. Medium density fibreboard (MDF) is a wood-based composite  
14 that is widely used in the furniture industry. The goal of the research conducted was to determine  
15 the effect of the type of coating on the drill cutting blades on the value of thrust force ( $F_t$ ), cutting  
16 torque ( $M_c$ ), cutting tool temperature ( $T$ ) and surface roughness of the hole in drilling MDF panels.  
17 In the tests three types of carbide drills (HW) were used: not coated, TiAlN coated and ZrN coated.  
18 The measurement of both the thrust force and the cutting torque was carried out using an industrial  
19 piezoelectric sensor. The temperature of the cutting tool in the drilling process was measured using  
20 an industrial temperature measurement system using a K-type thermocouple. It was found that the  
21 value of the maximum temperature of the tool in the drilling process depends not only on the cutting  
22 speed and feed rate, but also on the type of coating of the cutting tool. The value of both the cutting  
23 torque and the thrust force is significantly influenced by the value of the feed rate and the type of  
24 drill coating. The effect of varying plate density on the surface roughness of the hole and the  
25 variation of the value of the thrust force is also discussed. The results of the investigations were  
26 statistically analysed using a multi-factorial analysis of variance (ANOVA).

27 **Keywords:** drilling MDF; thrust force; cutting temperature; surface roughness; cutting tool coating

28

### 29 1. Introduction

30 Medium density fibreboard (MDF) is a wood-based product widely used in the furniture  
31 industry [1-5]. MDFs are composed of wood fibres, bonded with formaldehyde glue under the  
32 influence of heat and pressure. The use of medium density fibreboards in industry is associated with  
33 their machining during furniture production. One of the most commonly used operations in the  
34 production of MDF furniture is drilling. The MDFs machinability is determined by the quality of the  
35 surface [5, 6], which largely depends on the degree of tool wear and the mechanism of chip formation  
36 [7]. Various studies have been carried out to improve understanding of MDF cutting characteristics  
37 [4, 8-10]. Most of the studies are mainly focused on measuring the cutting forces and the friction  
38 phenomenon based on the theory used in the cutting process of metals [11, 12]. Cutting forces,  
39 temperature and surface roughness that reflect susceptibility to material processing are three  
40 important issues in the machining of wood-based materials. Cutting forces have a direct effect on  
41 energy consumption, tool wear, heat generation and the quality of the surface machined [13-15].

42 In order to maintain the relatively long service life of cutting tools used for MDF machining, it  
43 is necessary to use tools with a high wear resistance. Blades made from HM cemented carbide or  
44 diamond are the most commonly used in the machining of wood-based materials. In the literature

45 we can find the results of investigations aimed at increasing the durability of the cutting tool blades  
46 in the machining of wood-based composites. Numerous experiments are focused on increasing the  
47 durability of the cutting tool blades by applying various coatings to the blade surfaces in order to  
48 reduce their wear [16-22]. Recently, this field of research has been developing dynamically. However,  
49 the use of cutting tools with new coatings requires a number of tests, within which the quality of the  
50 surface machined, the cutting temperature and the cutting resistance are assessed. The drilling  
51 process in metals has been widely studied, and the results of these tests are well described in the  
52 literature, while the process of drilling MDF has not received much attention [5, 15, 23, 24].

53 The cutting process of wood-based materials is strictly dependent on their physical and  
54 mechanical properties. MDF has a more homogeneous structure than solid wood. While solid wood  
55 exhibits anisotropic properties, MDF consists of several isotropic layers [25] where the highest  
56 density is observed at the edges of the panel, and the lowest density is in the middle of the panel.

57 Gordon and Hilery [10] presented a brief overview of work on forecasting the cutting forces in  
58 MDF machining. These works described the general mechanics of MDF machining based on  
59 assumptions occurring in metalworking. Djouadi et al. [17] investigated the use of polycrystalline  
60 diamond (PCD) cutting blades in MDF machining. They concluded that the main benefit of using  
61 PCD is the extended durability of the cutting tool resulting from its greater hardness and better  
62 tribological properties compared to traditional tool materials. Davim [2] studied the effect of various  
63 cutting parameters on surface roughness in the MDF milling process using uncoated cutting tools.  
64 Similar studies were carried out by Sedlecký [23].

65 Szwajka and others [15] conducted investigations of the drilling of melamine faced chipboard  
66 using a carbide drill. They developed an analytical model for predicting the effect of drilling  
67 parameters on thrust force. It was found that an increase in the value of the feed rate increases  
68 delamination of the chipboard.

69 The quality of the MDF surface is an important factor influencing the final appearance of the  
70 product or subsequent technological processes, such as gluing (adhesion and cohesion), coating,  
71 varnishing, etc. [23, 26]. The surface roughness of the surface machined depends on various factors  
72 and conditions [2, 24, 27], which can be classified as follows: type of machining (cutting, milling,  
73 drilling, etc.) [28-30], machining parameters (cutting speed, feed rate) [31-34], type of cutting tool  
74 (geometry, applied coatings on the cutting edge), as well as the properties of the material being  
75 processed [26].

76 Even if the machining parameters are the same, each machining method leaves characteristic  
77 irregularities on the surface; for example, saw cut surfaces differ from milled surfaces [8, 33]. The  
78 requirements for surface roughness are determined in accordance with the functional application of  
79 the future product [36, 37]. The surface roughness is determined by specifying the numerical value  
80 of one or several surface roughness parameters and the value of the sampling length [23].

81 Lin et al. [36] analysed the machinability of MDFs. They used a digital camera to record chip  
82 formation occurring in front of the cutting tool edge and a scanning electron microscope (SEM) for  
83 additional analysis of the surface machined. Davim et al. [38] studied the cutting parameters  
84 (cutting velocity and feed rate) under specific cutting pressure, thrust force, damage and surface  
85 roughness in glass fibre reinforced plastics. It was shown that the differences in MDF panel density  
86 are closely related to machinability characteristics.

87 The heat generated in the drilling process has a direct effect on the surface roughness of the  
88 surface machined, hole quality and chip morphology [1, 39]. The temperature in the region of contact  
89 of the blade with the material processed (wood or wood-based material) depends both on the energy  
90 released in this region and the efficiency of heat removal in this region. In addition to radiation,  
91 conductivity is the main mechanism responsible for heat removal. Considering the fact that the  
92 thermal conductivity of wood and wood-based materials is very low, and the use of cooling liquids  
93 is excluded, the main element responsible for heat removal is the tool. This leads to an undesirable  
94 increase in tool blade temperature. During the drilling process, the most important factor affecting  
95 the cutting output is the temperature created between the cutting tool and the workpiece. In this  
96 paper the effect that the type of coating on the drill cutting blades has on the value of thrust force,

97 cutting torque, cutting tool temperature and surface roughness of the hole in drilling MDF panels is  
 98 investigated. Three types of carbide drills (HW) were used in the tests: not coated, TiAlN coated and  
 99 ZrN coated.

## 100 2. Experimental Procedure

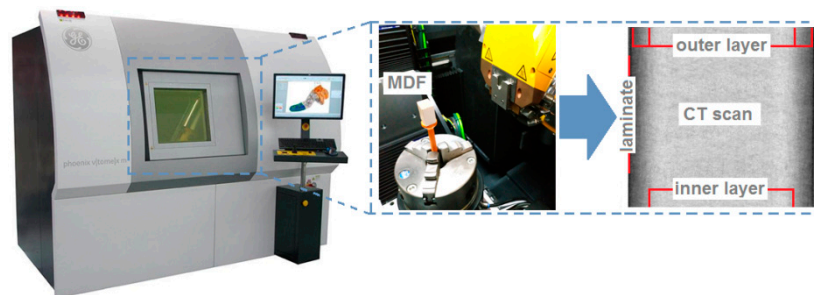
### 101 2.1. Material

102 A typical industrial MDF panel with a thickness of 18 mm was used as the workpiece. The  
 103 mechanical and physical properties of the material being processed are listed in Table 1. An MDF  
 104 panel is characterised by a clear differentiation of material density in the cross-section, which results  
 105 from its multi-layered structure. To more accurately characterise the workpiece, a laboratory  
 106 measurement of the density profile through the panel thickness was carried out using a Phoenix v-  
 107 tomome x-ray tomograph (GE Sensing & Inspection Technologies, Wunstorf, Germany).

108 **Table 1.** Selected mechanical and physical properties of MDF.

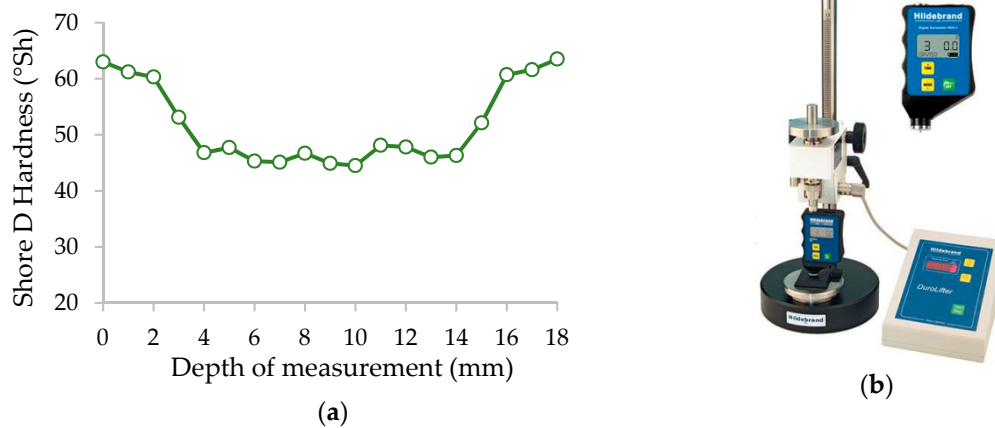
Density (kg/m <sup>3</sup> )	Moisture content (%)	Bending Strength (MPa)	Elasticity Modulus (MPa)	Thermal Conductivity (W/m*K)	Thermal Expansion ( $\mu\text{m}/\text{m}^*\text{K}$ )
742	7.2	38	2530	0.3	12

109 X-ray tomographs permits one to obtain tomographic images of the object examined, and then  
 110 present its spatial (3D) image from many flat (2D) images taken in various positions. The computer  
 111 tomographic (CT) images contain information about the location and density of the absorbing  
 112 features in the object. Any difference in material density inside the object can be measured and  
 113 visualised. Figure 1 shows a picture of the cross-section of an MDF panel, in which a distinct variation  
 114 in plate density can be observed. The highest density occurs in the outer layers of the panel (to a  
 115 depth of about 2.3 mm). However, a lower density appears in the inner layer (around 13.4 mm in  
 116 length) (Figure 1).



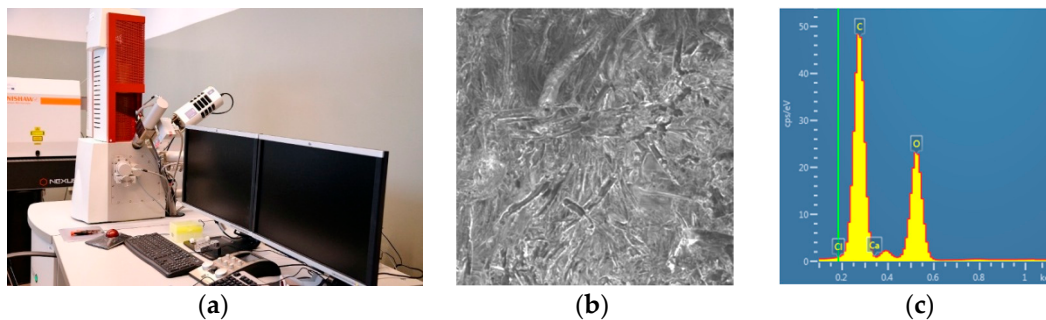
117 **Figure 1.** MDF density measurement on a computer tomography Phoenix v|tome|x m.

118 Furthermore, the hardness distribution of the material processed was measured using a Shore  
 119 hardness tester (Hildebrand, Oberboihingen, Germany) using the Shore D scale (Figure 2b). As can  
 120 be seen, the hardness distribution (Figure 2a) is closely related to the density profile. The highest  
 121 hardness value occurs in the outer layers with a thickness of approximately 2.3 mm and is equal to  
 122 62°Sh (D scale). As we move away from the outer layer, the hardness decreases, reaching a value of  
 123 43°Sh (D scale) at a depth in the range between 7 mm and 11 mm.



124 **Figure 2.** Hardness measurement: (a) Hardness profile of MDF used in tests; (b) Shore hardness  
125 tester.

126 The spectral analysis of the elements constituting the material (Figure 3) was carried out using  
127 a scanning electron microscope (TESCAN, MIRA3, Brno, Czech Republic).



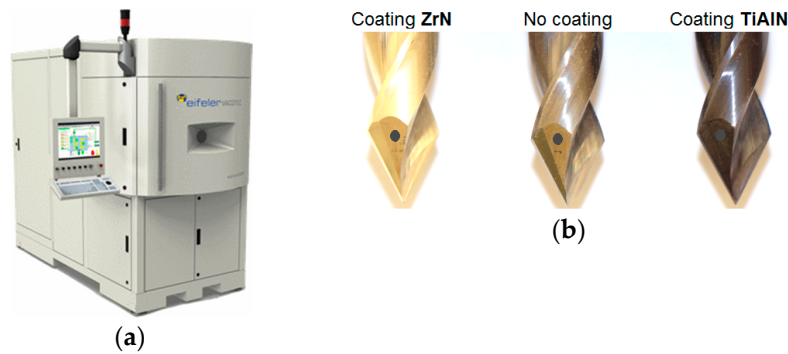
128 **Figure 3.** Scanning electron microscope and spectral analysis of the MDF: (a) Measuring stand; (b)  
129 Microphotograph of an MDF panel surface; (c) Spectra of the outer surface of an MDF panel.

## 130 2.2. Cutting tools

131 In the drilling of MDFs, HW sintered carbide cutting tools were used with different types of  
132 cutting blade coating. Two types of coating for cutting blades, i.e. TiAlN and ZrN were used. The  
133 selection of coatings was dictated by the fact that they belong to those most commonly used in the  
134 machining of composite materials [40]. In the case of cutting wood-based materials, there is a general  
135 lack of commercially available cutting tools (especially drills) with additional protective coatings. In  
136 the research it was necessary to measure the temperature of the cutting blade during the drilling  
137 process. To measure the temperature between the cutting edge and the workpiece using  
138 thermocouples, it was necessary for the tool to have coolant channels. However, no cooling liquids  
139 are used in the treatment of MDFs. So, it was necessary to fabricate drills. The geometry of the drills  
140 was based on the geometry of the Leitz® HW / D10 / NL35 / S10x24 / GL70 drill (Leitz GmbH & Co.  
141 KG, Oberkochen, Baden-Württemberg, Germany), which is widely used in the drilling of through-  
142 holes in MDFs.

143 A coordinate measuring machine is used to measure the geometrical dimensions of the reference  
144 tool in order to make drills with coolant channels identical to the standard ones but made of cemented  
145 carbide monolith, which will be covered with two different coatings. The Zoller® Genius 3 coordinate  
146 measuring machine (Zoller, USA) (Figure 4) was used to measure and control the geometry of the  
147 cutting tools. This machine is used by tool manufacturers to enable one to take measurements in a  
148 fully automatic way. Fully automatic precise measurements are assured by 5 numerically controlled  
149 axes (X, Y, Z, C, B).





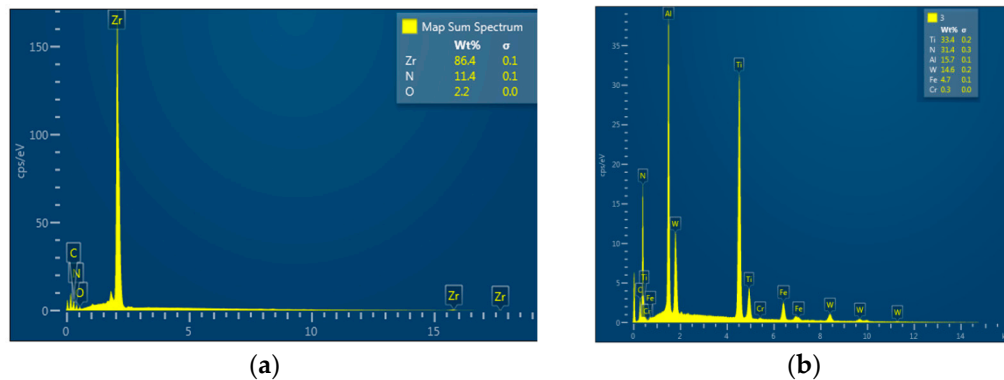
177 **Figure 6.** Stand for applying protective coatings: (a) Vacuum reactor EIFELER VACOTEC PVD Alpha  
 178 400 ; (b) Drills with the coatings used in the research.

179 The coatings were made on a substrate previously sprayed with high energy ions, free of oxides  
 180 and enriched with elements forming a strong adhesion-diffusion bond. The selected properties of the  
 181 coatings used are listed in Table 2.

182 **Table 2.** Selected mechanical and physical properties of the coatings.

Type of coating	Coating Temperature (°C)	Hardness (HV)	Thickness (µm)	Coefficient of Friction	Thermal Conductivity (W/m*K)
ZrN	350-500	2200	2-3	0.4	0.28
TiAlN	400-500	3000	2-3	0.6	2.48

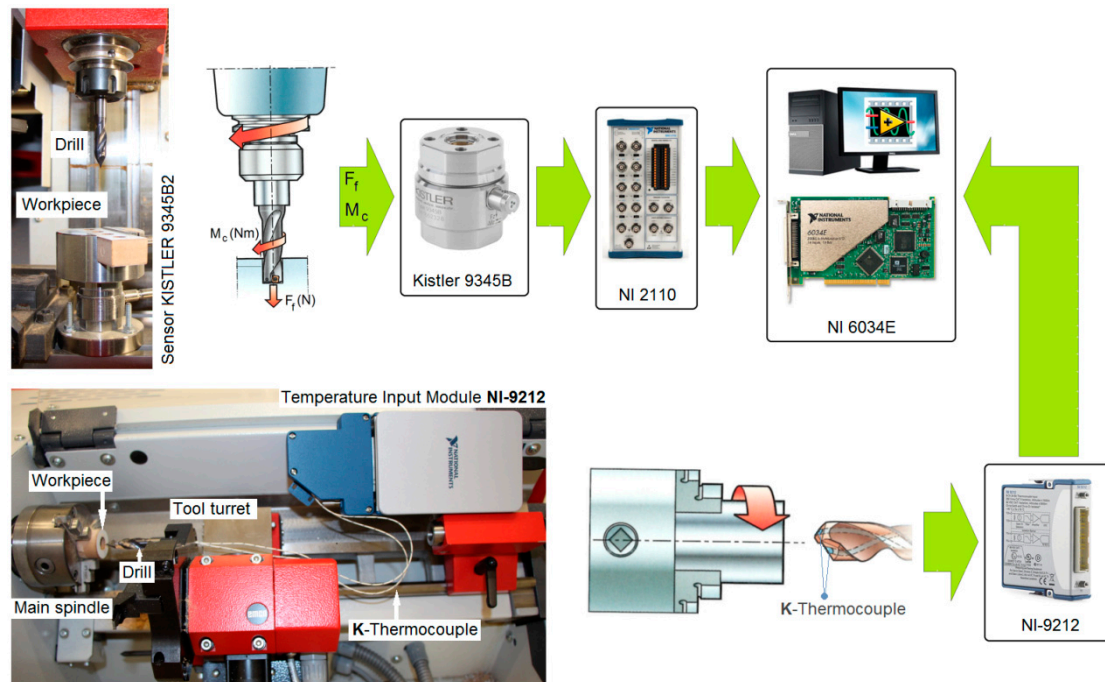
183 Three types of drills with coolant channels were fabricated: an HW carbide drill with a ZrN  
 184 coating, an HW carbide drill without a coating and an HW carbide drill with a TiAlN coating (Figure  
 185 6b). The spectral analysis of the elements included in the coating applied (Figure 7) was carried out  
 186 using a TESCAN® scanning electron microscope (TESCAN, MIRA3, Brno, Czech Republic).



187 **Figure 7.** Results of spectral analysis of the drills: (a) ZrN coated drill; (b) TiAlN coated drill.

### 188 2.3. Equipment and Machining Conditions

189 The drilling process was carried out in two stages: on a CNC vertical milling machine and on an  
 190 EMCO® CNC lathe (EMCO GmbH, Hallein, Austria). A schematic diagram of the configuration of  
 191 the measurement path and the measurement data archiving system is presented in Figure 8. In the  
 192 first stage of testing, the CNC milling machine recorded the values of thrust force ( $F_t$ ) and cutting  
 193 torque ( $M_c$ ) during MDF machining.



194  
195

**Figure 8.** Experimental set-up and schematic diagram of the data acquisition system.

196 In the first stage, three holes (with the same set of cutting parameters) were drilled in an MDF  
197 panel with dimensions  $130 \times 30 \times 18$  mm on a CNC milling machine. The value of the thrust force and  
198 the cutting torque was measured using the Kistler® 9345B2 piezoelectric industrial sensor (Kistler,  
199 Winterthur, Switzerland). The signals from the sensor were recorded on a personal computer (PC)  
200 disk via the National Instruments® 6034E (Austin, TX, USA) 16-bit analogue-to-digital card with a  
201 sampling rate of 50 Hz. The surface topography of each completed hole was measured in two  
202 locations (every  $180^\circ$ ) using the Hommel-Etamic T8000RC CNC profilometer (Jenoptik, Jena,  
203 Germany) (Figure 9). In order to measure the surface roughness, the test sample was cut into two  
204 parts along the hole axis. One measurement was made for each part separately.

205  
206

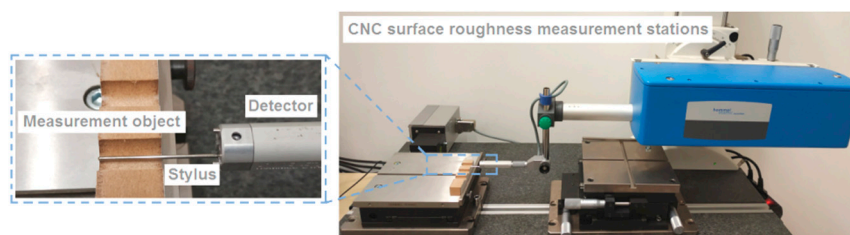
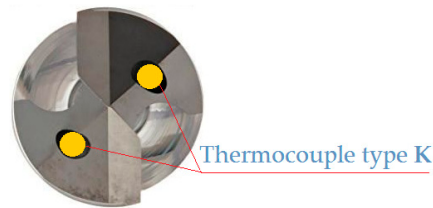


**Figure 9.** Measurement of surface topography.

207 In the second stage of the investigations, the holes were drilled (with the same set of cutting  
208 parameters) in MDF workpieces with a diameter of 30 mm and a thickness of 18 mm on a CNC lathe.  
209 The temperature value was measured during machining between the cutting edge and the workpiece  
210 using the National Instruments® 9212 industrial system (Austin, TX, USA). Two K-type  
211 thermocouple wires with a diameter of 0.2 mm were used for temperature measurement. The  
212 thermocouple wires were mounted in the cooling liquid drill channels (Figure 10). Signals from the  
213 measurement system were recorded in digital form on a personal computer (PC) disk. The sampling  
214 rate of signals during experiments was 5 Hz, and a 24-bit measurement card was used.



215  
216

**Figure 10.** Drill with inserted thermocouples.

217 The cutting parameters used during the drilling experiments are listed in Table 3. Three  
218 replications were made for each of the sets of cutting parameters. This research methodology was  
219 applied to drilling with the following types of drills: not coated, ZrN coated and TiAlN coated.

220

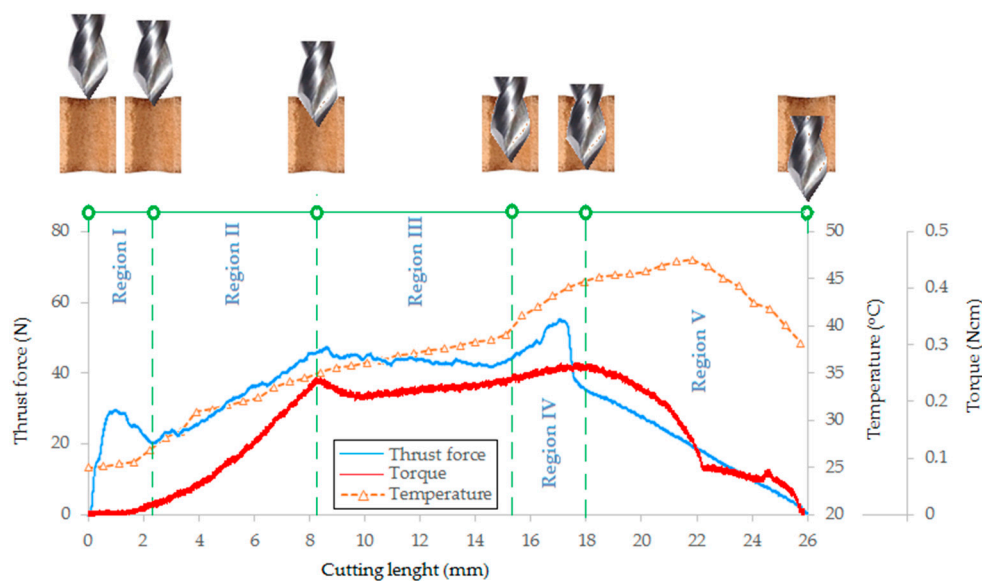
**Table 3.** Machining conditions.

Cutting speed (m/min)	Feed per revolution (mm/rev)	Feed rate (mm/min)	Rotational speed of drill (rev/min)
35	0.10	111	1114
35	0.15	167	1114
35	0.20	222	1114
70	0.10	222	2229
70	0.15	334	2229
70	0.20	445	2229
105	0.10	334	3344
105	0.15	501	3344
105	0.20	668	3344

## 221 3. Results

### 222 3.1. Feed force and cutting torque

223 Figure 11 shows the variation in thrust force, cutting torque and cutting edge temperature as a  
224 function of cutting length when drilling the MDF at a cutting speed of 35 m/min and a feed rate of  
225 167 mm/min using the TiAlN coated drill.



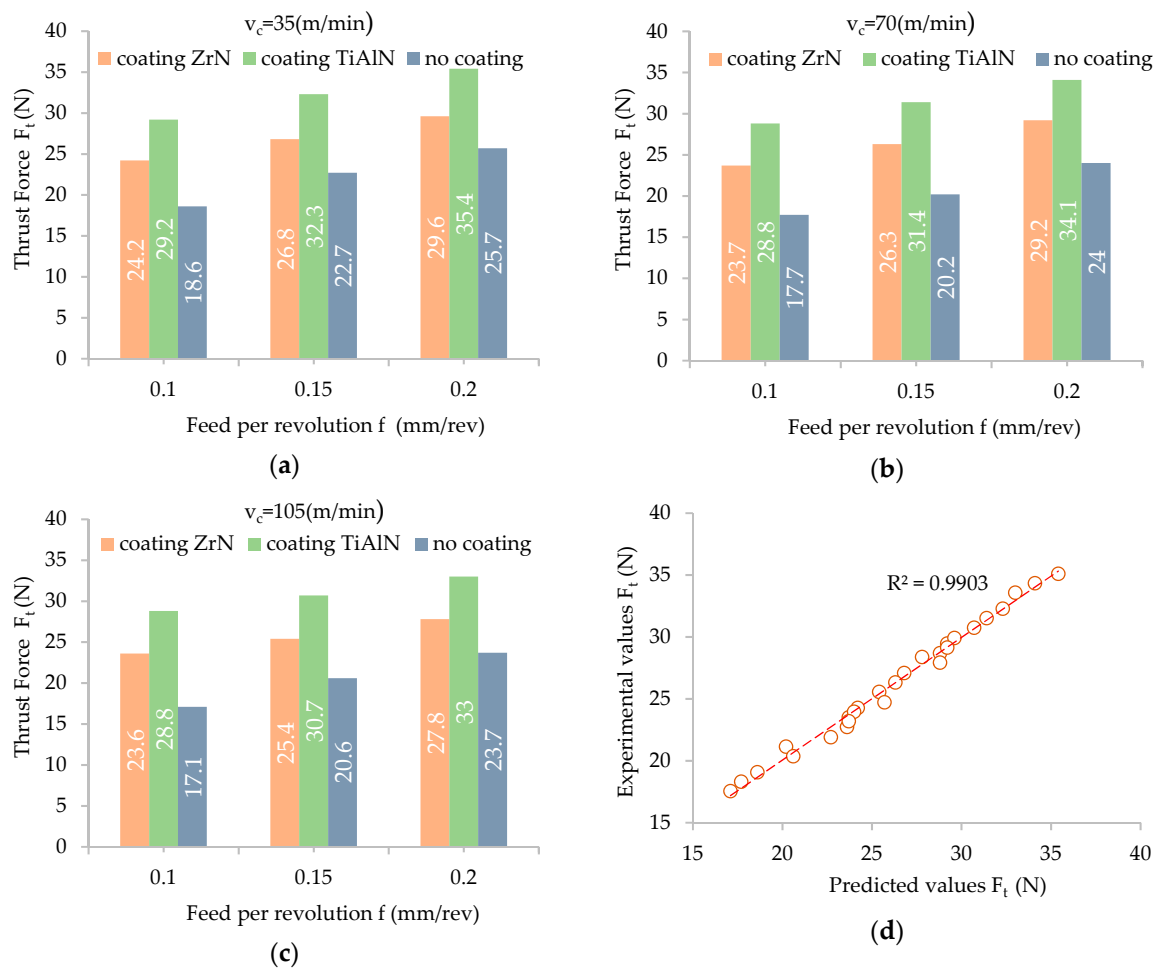
226  
227

**Figure 11.** Variation of thrust force, cutting torque and temperature in the drilling process.

228 It was observed that five major phases of the variation of the thrust force ( $F_t$ ) value can be  
229 identified during drilling (Regions I-V in Figure 11). In the period referred to as Phase I, the chisel  
230 edge of the drill penetrates into the material producing a rapid increase in the value of the thrust  
231 force. During this phase, instead of cutting, the chisel edge of the drill is pressed into the material.  
232 Then the drill starts to cut the outer layer of the material with the highest density and hardness. When  
233 the chisel edge of the drill leaves the area of material with the highest density (depth approx. 2.2 mm),  
234 the force value decreases due to the fact that the drill sinks into the middle layer of the panel with  
235 lower density and hardness. During Phase II the drill penetrates to a depth of  $h = 8.1$  mm, which is  
236 equal to the height of the cutting blades of the drill (Figure 5c). During this time, there is an increase  
237 in the cross-sectional area of the cutting layer, which results in a proportional increase in the thrust  
238 force. Phase III corresponds to cutting with a constant cross-section of the cutting layer in the middle  
239 layer of the panel. Stabilisation of the thrust force value is then observed. At the beginning of Phase  
240 IV, the value of the thrust force starts to increase rapidly due to the fact that the drill begins to  
241 penetrate the outer layer of the material (higher density and hardness). The thrust force reaches its  
242 maximum value. When the chisel edge of a drill leaves the workpiece (cutting path approx. 18 mm),  
243 the thrust force starts to decrease (Phase V). The value of the thrust force drops to zero at the end of  
244 Phase V when the cutting edges of the drill have left the workpiece.

245 In the case of cutting torque ( $M_c$ ), it is clearly visible in Phase I that there is no machining, and  
246 only the chisel edge of a drill is pressed into the workpiece. In Phase I the cutting torque value is close  
247 to zero. Next, the blades sink into the workpiece (Phase II) which results in a proportional increase  
248 in the value of cutting torque. The period of this increase continues until the drill reaches the  
249 maximum cross-sectional area of the cutting layer, i.e. the drill is penetrated to a depth of  $h = 8.1$  mm.  
250 In Phase III, the cutting of the cutting layer with a constant cross section in the middle layer of the  
251 panel proceeds. A stabilisation of the cutting torque value is observed. At the beginning of Phase IV  
252 the value of the cutting torque starts to increase due to the fact that the drill begins to enter into the  
253 outer layer of material (higher density and hardness). Furthermore, in this phase the largest cross-  
254 section of the material is cut and the cutting torque reaches its maximum value. When the drill begins  
255 to come out of the workpiece (cutting path approx. 18 mm), the cutting torque starts to decrease  
256 (Phase V). In the middle part of Phase V, some stabilisation of the cutting torque is observed. As a  
257 result the drill that comes out of the material cuts only the outer layer of the material characterised  
258 by high density and hardness. The cutting torque value drops to zero at the end of Phase V when the  
259 cutting edges of the drill have left the workpiece. For the analysis of the acquired signals of  $F_t$  and  
260  $M_c$ , an individually designed computer program was prepared in the LabVIEW programming  
261 language enabling, at selected time intervals, the mean values of the recorded thrust force and cutting  
262 torque signals to be determined. The program was based on the automatic determination of values  
263 of  $F_t$  and  $M_c$  parameters in a specific time range of the signal. The methodology for determining the  
264 average values of recorded signals has been described in detail in [5]. Figures 12a-c show the effect  
265 of feed per revolution ( $f$ ) on the thrust force ( $F_t$ ) for the three cutting speeds and the three types of  
266 drill coating. The thrust force values presented in the graphs were obtained as the average result of  
267 three repetitions.

268 Multi-factorial analysis of variance (ANOVA) carried out in the STATISTICA program allowed  
269 the verification of the significance of the influence of several independent variables on the dependent  
270 variable. Furthermore, multivariate analysis makes it possible to take the synergistic effect of the  
271 product of many variables into account in the statistical model. Taking into account the adopted level  
272 of significance of  $p = 0.05$ , the statistical significance of particular groups of variables and individual  
273 variables is determined. The results of the analysis (Table 4) allow one to reject, at a significance level  
274  $p = 0.000$ , the hypothesis concerning the lack of effect of the factors "coating", feed per revolution ( $f$ )  
275 and cutting speed ( $v_c$ ) on the value of the thrust force ( $F_t$ ). There was no statistically significant effect  
276 of interactions between the factors analysed.



277 **Figure 12.** Influence of the feed value on the value of the thrust force: (a) for cutting speed 35 m/min;  
 278 (b) for cutting speed 70 m/min; (c) for cutting speed 105 m/min; (d) correlation between the  
 279 experimental and predicted values of thrust force.

280 **Table 4.** Significance level of the effect of cutting parameters on the average thrust force ( $F_t$ ).

Tests Applied	Level of Significance ( $p \leq 0.05$ )
cutting speed ( $v_c$ )	0.000
feed per revolution ( $f$ )	0.000
coating	0.000
coating*cutting speed	0.997
coating*feed per revolution	0.564

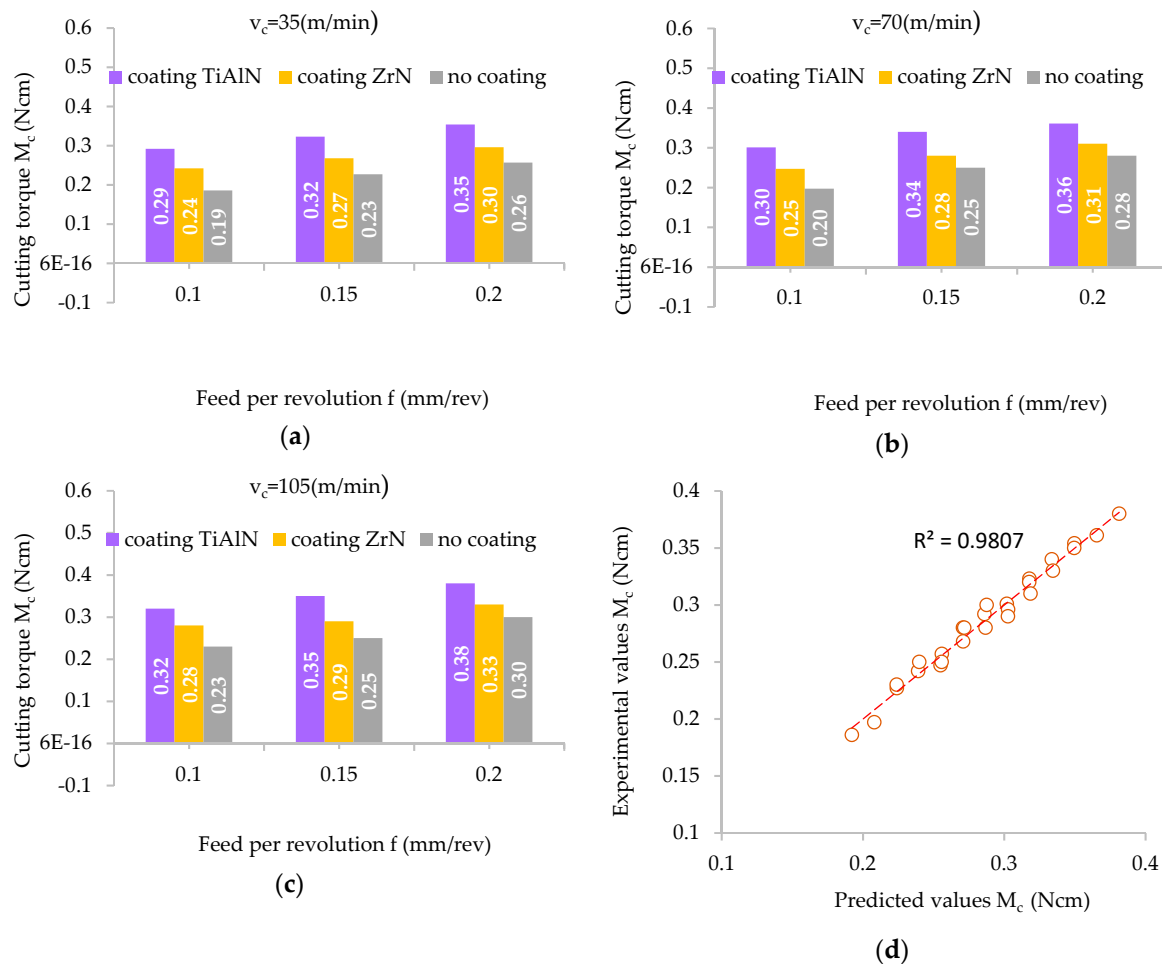
281 The smallest value of thrust force ( $F_t$ ) was obtained in the drilling process using a tool without  
 282 a coating. However, the highest values of thrust force were obtained for a drill with a TiAlN coating.  
 283 The increase in the value of the thrust force in comparison to machining without a coating was on  
 284 average about 39%. In the case of a ZrN coated drill, the value of the thrust force obtained was  
 285 reduced in comparison to the TiAlN coated drill, but it was still higher on average by about 17% in  
 286 relation to the value obtained with the use of a drill without a coating. For example: for the cutting  
 287 speed  $v_c = 105$  m/min and feed per revolution value  $f = 0.2$  mm/rev the value of the thrust force for  
 288 the TiAlN coated drill was 33 N, for the tool with a ZrN coating was 27.8 N and for the tool without  
 289 a coating it was 23.7 N. This can be explained by the differing values of the coefficient of friction  
 290 between the tool and the workpiece material resulting from the type of coating used. For all the  
 291 coatings used, the value of the thrust force increases with an increase in the value of the feed per  
 292 revolution. The value of the thrust force can be described by the equations (1-3).

$$F_t \text{ (N)} = 25.139 + 52.333*f - 0.021*v_c, \text{ (ZrN)} \quad (1)$$

$$F_t \text{ (N)} = 20.005 + 50.333*f - 0.018*v_c, \text{ (TiAlN)} \quad (2)$$

$$F_t \text{ (N)} = 13.011 + 66.667*f - 0.026*v_c, \text{ (no coated)} \quad (3)$$

293 Figure 12d presents a comparison between the results for the values of the thrust force obtained  
 294 during the experiment with the values obtained based on the analytical model (1). The correlation  
 295 coefficient obtained was equal to  $R^2 = 0.9903$ . Figures 13a-c shows the relations of cutting material  
 296 ( $M_c$ ) versus the feed per revolution ( $f$ ) for the three cutting speeds ( $v_c$ ) and three types of drill coatings.  
 297 The influence of these parameters on the cutting torque ( $M_c$ ) is noticeable to a lesser extent.



298 **Figure 13.** Influence of the feed value on the value of the cutting torque: (a) for cutting speed 35 m/min;  
 299 (b) for cutting speed 70 m/min; (c) for cutting speed 105 m/min; (d) correlation between experimental  
 300 and predicted values of cutting torque.

301 The results of the statistical analysis (Table 5) allow one to reject, at the level of significance  $p =$   
 302 0.000, the hypothesis that the coating type, feed per revolution ( $f$ ) and cutting speed ( $v_c$ ) do not affect  
 303 the value of the cutting torque ( $M_c$ ). In the case of interactions between the factors analysed, no  
 304 statistically significant effect of these factors on the value of ( $M_c$ ) was observed.  
 305

306

**Table 5.** Significance level of the effect of cutting parameters on the average cutting torque ( $M_c$ ).

Tests Applied	Level of Significance ( $p \leq 0.05$ )
cutting speed ( $v_c$ )	0.000
feed per revolution ( $f$ )	0.000
coating	0.000
coating*cutting speed	0.853
coating*feed per revolution	0.734

307

308

309

310

311

312

313

The lowest value of torque was obtained using the drill without a coating in the drilling process (Figure 13). The highest values of cutting torque ( $M_c$ ) recorded in the experiments were obtained using a drill with a TiAlN coating. The increase in the value of cutting torque when machining using coated drills in comparison to that using an uncoated drill was approximately 35%. In the case of a ZrN coated drill, the value of the cutting torque ( $M_c$ ) obtained was less than that using a TiAlN coated drill, but it was still greater by approx. 15% in relation to the value of ( $M_c$ ) obtained with a drill without a coating.

314

315

316

317

318

319

320

321

For example: for the cutting speed  $v_c = 35$  m/min and feed per revolution value  $f = 0.2$  mm/rev the cutting torque ( $M_c$ ) for the TiAlN coated drill was 0.35 Ncm, for the ZrN coated drill it was 0.3 Ncm and for the drill without coating was 0.26 Ncm. In a similar manner to the effect of drilling parameters on the value of the thrust force, this fact can be explained by the differing values of the coefficient of friction between the tool and the workpiece resulting from the type of drill coating. For all the coatings used, the value of the thrust force ( $F_t$ ) increases with an increase of the feed per revolution ( $f$ ) value. The value of the thrust force ( $F_t$ ) can therefore be described by the equations (4-6).

$$M_c \text{ (Ncm)} = 0.218 + 0.607*f - 0.001*v_c, \text{ (ZrN)} \quad (4)$$

$$M_c \text{ (Ncm)} = 0.167 + 0.557*f - 0.001*v_c, \text{ (TiAlN)} \quad (5)$$

$$M_c \text{ (Ncm)} = 0.093 + 0.747*f - 0.001*v_c, \text{ (no coated)} \quad (6)$$

322

323

324

325

326

Figure 13d shows a comparison of the results of the cutting torque values obtained during the experiment with the values obtained on the basis of the analytical model. A correlation coefficient  $R^2 = 0.9807$  was obtained between the experimental and predicted values of cutting torque ( $M_c$ ). For all the coatings of tools used, the value of the cutting torque ( $M_c$ ) increases as the feed per revolution ( $f$ ) increases.

327

### 3.2. Analysis of Surface Topography

328

329

330

331

332

333

334

335

Surface topography is one of the main features taken into account to evaluate the surface quality in machining processes. The value of the roughness average  $R_a$  parameter was measured in the longitudinal direction of the holes machined in MDF panels. The choice of this indicator to assess surface roughness was dictated by its very frequent use in production plants [23]. The value of the roughness average ( $R_a$ ) was determined on the basis of the surface topography map in selected measurement sections. Figures 14a-c show an example of the topography of the hole surface obtained in the process of drilling with a TiAlN coated drill at a cutting speed of 105 m/min and with three feed per revolution values.

336

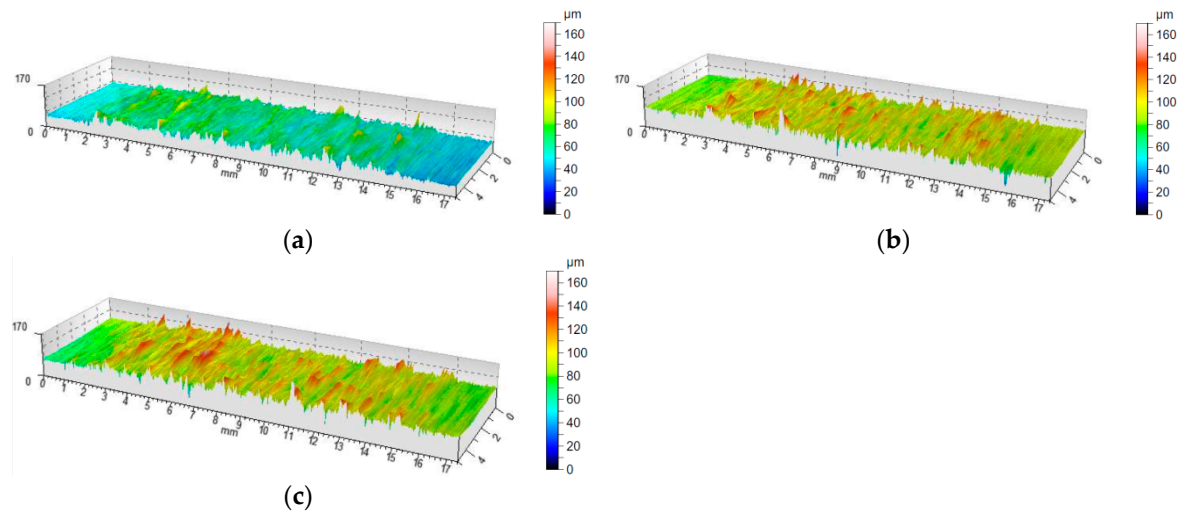
337

338

339

340

Three areas with a different character of surface roughness can clearly be seen on the surface topographies presented. The first and the second area occur in the outer layers of the MDF panel and the third area in the middle layer of the board. This diversity can be explained by the abovementioned multi-layered structure of the MDFs. The resulting surface topography accurately reflects changes in both hardness and panel density.



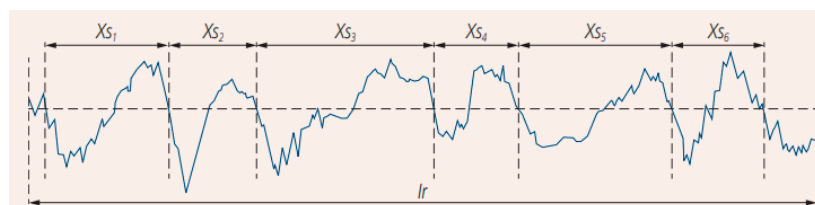
341 **Figure 14.** The topography of the surface drilled with a TiAlN coated tool: (a) cutting speed 105 m/min  
 342 and feed per revolution 0.1 mm/rev; (b) cutting speed 105 m/min and feed per revolution 0.15 mm/rev;  
 343 (c) cutting speed 105 m/min and feed per revolution 0.2 mm/rev.

344 Measurement of the roughness average (Ra) parameter was carried out in accordance with the  
 345 recommendations of ISO-4288:2011. The test conditions of the surface roughness measurement were  
 346 adopted in accordance with Table 6. The mean groove spacing (RSm) value (Figure 15) in the  
 347 measurements was in the range between 0.13 and 0.4.

348 **Table 6.** Setup for the roughness measurement (EN ISO 4288).

Mean Groove Spacing for Periodic Profiles RSm (mm)	Measurement parameter			
	$\lambda_c = l_c$ (mm)	$l_n$ (mm)	$l_t$ (mm)	$r_{tip}$ ( $\mu\text{m}$ )
$0.013 < R_{Sm} \leq 0.04$	0.08	0.4	0.48	2
$0.04 < R_{Sm} \leq 0.13$	0.25	1.25	1.5	2
$0.13 < R_{Sm} \leq 0.4$	0.8	4	4.8	2 or 5
$0.4 < R_{Sm} \leq 1.3$	2.5	12.5	15	5
$1.3 < R_{Sm} \leq 4$	8	40	48	10

349  $r_{tip}$  maximum probe tip radius,  $l_r$  sampling length,  $l_n$  evaluation length,  $l_t$  stylus travel  
 350 (evaluation.length plus start and finish lengths).

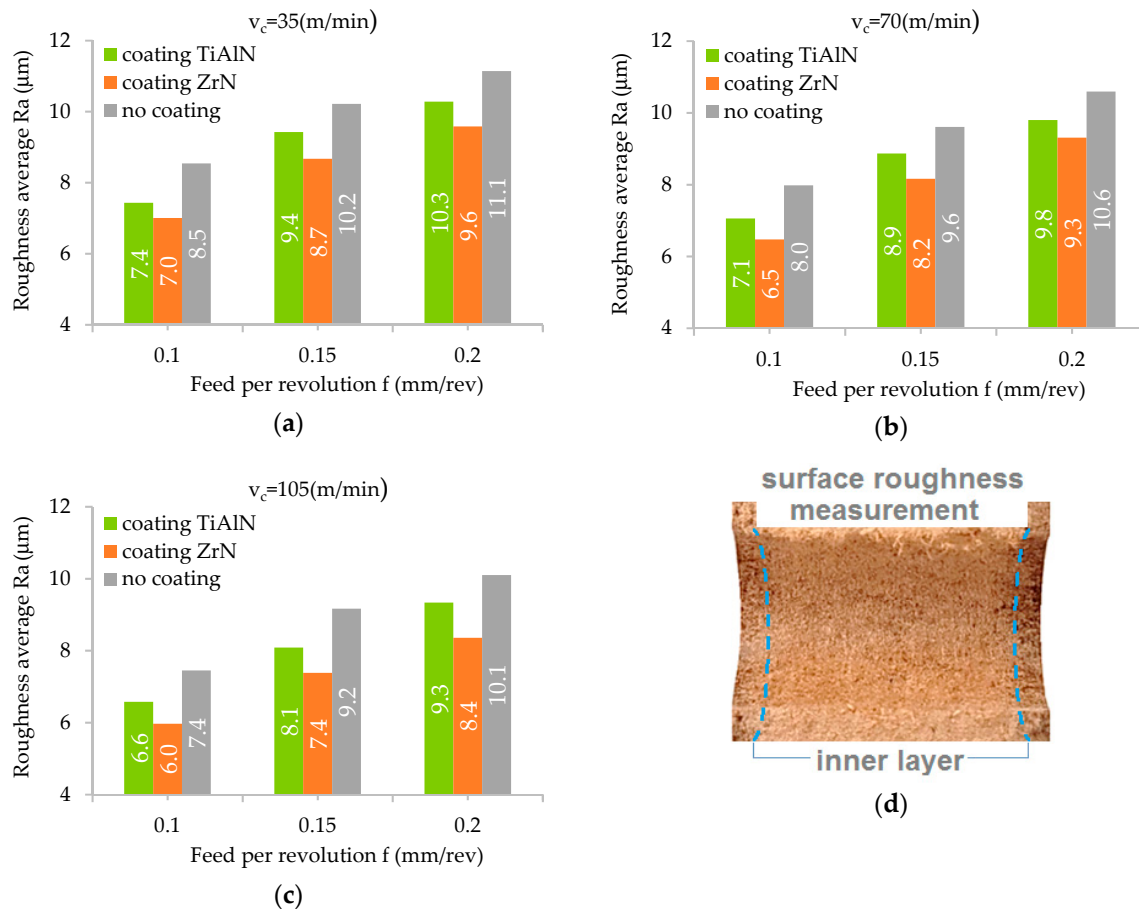


351 **Figure 15.** The mean groove spacing RSm as the mean value of the spacing  $X_{Si}$  of the profile  
 352 elements.  
 353

354 The value of the Ra roughness average parameter was determined separately for the outer layer  
 355 and middle layer of the MDF. Therefore, the additional effect of both the density and hardness of the  
 356 workpiece on the Ra parameter can be analysed.

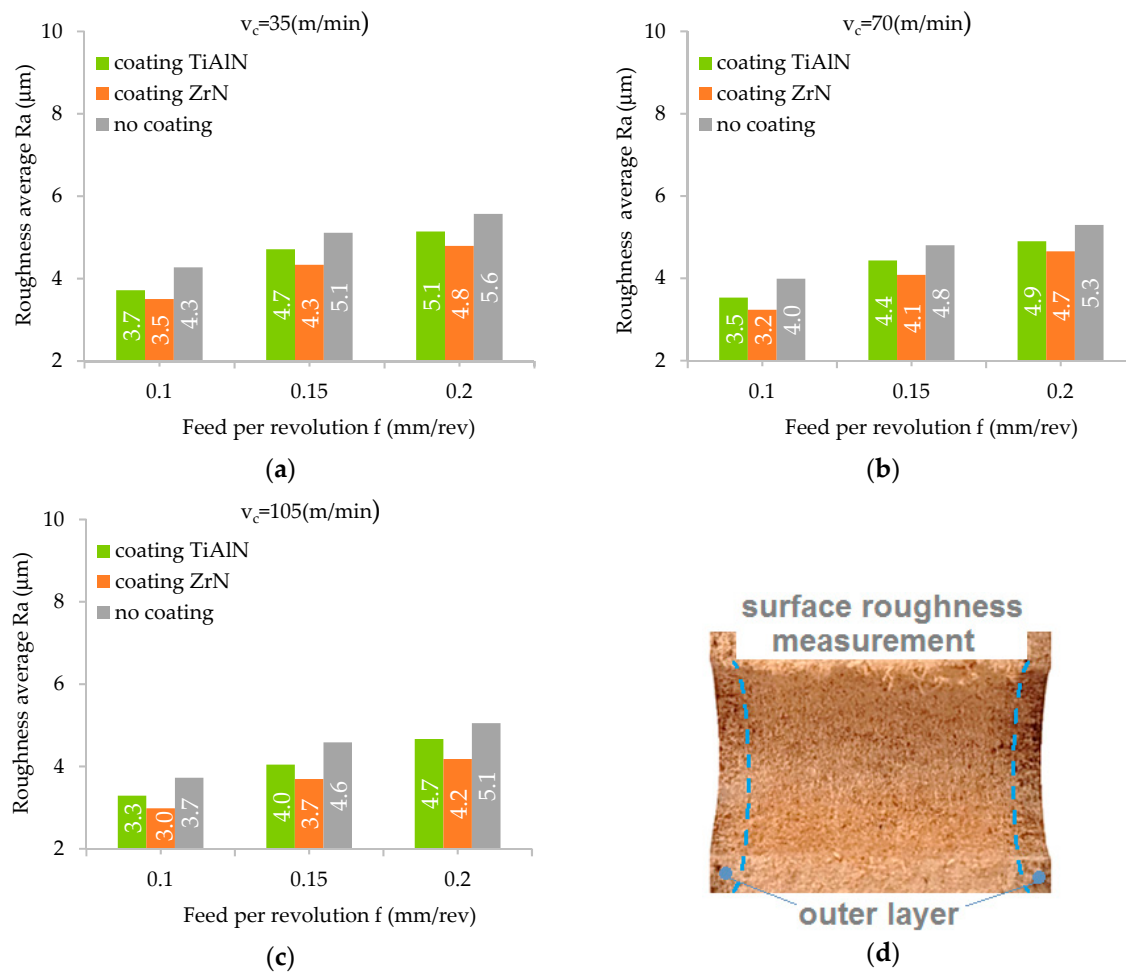
357 Figures 16 and 17 show the effect of the feed per revolution value for the three cutting speeds  
 358 and all types of tool coatings. The values of roughness average (Ra) in Figures 16 and 17 are the  
 359 average of six measurements. As mentioned, two measurements were made for each hole, and the

360 drilling of each hole was repeated three times. The results presented in Figure 16 refer to the  
 361 measurement of the surface roughness in the middle layer of the workpiece.



362 **Figure 16.** Influence of the feed value on the value of the surface roughness in the inner layer: (a) for  
 363 a cutting speed of 35 m/min; (b) for a cutting speed of 70 m/min; (c) for a cutting speed of 105 m/min;  
 364 (d) measurement area.

365 Figure 17 presents the results regarding the measurement of surface roughness in the outer layer  
 366 of the workpiece. In both cases, as the cutting speed ( $v_c$ ) increases and simultaneously the feed per  
 367 revolution ( $f$ ) decreases, the value of the roughness average ( $R_a$ ) decreases. For the inner layer of  
 368 panel at a cutting speed of 35 m/min and a feed per revolution of 0.2 mm/rev, the roughness average  
 369 parameter was  $R_a = 10.3 \mu\text{m}$  for a TiAlN coated drill, for a cutting speed of 105 m/min and a feed per  
 370 revolution of 0.1 mm/rev, the roughness average parameter was  $R_a = 6.6 \mu\text{m}$ . However, for the outer  
 371 layer of the panel at a cutting speed of 35 m/min and a feed per revolution of 0.2 mm/rev, the  
 372 roughness average parameter was  $R_a = 5.1 \mu\text{m}$ , while for a cutting speed of 105 m/min and a feed per  
 373 revolution of 0.1 mm/rev the roughness average parameter was  $R_a = 3.3 \mu\text{m}$  for a drill with TiAlN  
 374 coating. This can be explained by the fact that the accumulation of chips in the chip spaces decreased  
 375 with increasing cutting speed ( $v_c$ ). In addition, the very pronounced impact of the type of tool coating  
 376 on the surface roughness value was noted. It has been found that machining with a ZrN coated tool  
 377 allows one to achieve the lowest surface roughness value compared to a TiAlN coated tool and an  
 378 uncoated tool. This may be caused by a different value of friction coefficient as well as of thermal  
 379 conductivity coefficient depending on the type of coating (Table 2). A higher value of friction  
 380 coefficient and a lower value of coefficient of thermal conductivity causes an increase in the  
 381 temperature value in the tool-workpiece contact area. The increase in heat generated in the area of  
 382 contact between the cutting tool and the workpiece, in the case of MDF, significantly improves the  
 383 connection of wood fibres and formaldehyde adhesive. It causes the compaction of the bonds  
 384 between fibres.



385 **Figure 17.** Influence of the feed value on the value of the surface roughness in the outer layer: (a) for  
 386 a cutting speed of 35 m/min; (b) for a cutting speed of 70 m/min; (c) for a cutting speed of 105 m/min;  
 387 (d) measurement area.

388 The results of the analysis (Table 7) allow one to reject, at a significance level  $p = 0.000$ , the  
 389 hypothesis that the coating type and feed per revolution ( $f$ ) do not affect the  $R_a$  parameter value.  
 390 There was no statistically significant impact of the cutting speed ( $v_c$ ) on the  $R_a$  parameter value.  
 391 Similarly, in the case of interactions between the factors analysed, no statistically significant impact  
 392 was observed.

393 **Table 7.** Significance level of the effect of cutting parameters on the roughness average ( $R_a$ ).

Tests Applied	Level of Significance ( $p \leq 0.05$ )
cutting speed ( $v_c$ )	0.252
feed per revolution ( $f$ )	0.000
coating	0.000
coating*cutting speed	0.999
coating*feed per revolution	0.998

394 The experiments conducted showed that the feed per revolution ( $f$ ) value, cutting speed ( $v_c$ ) and  
 395 the type of tool coating have a significant influence on the roughness average ( $R_a$ ) parameter.  
 396 However, the  $R_a$  parameter values measured in the outer layers are significantly lower than those  
 397 measured in the inner layer.

398 3.3. Temperature of cutting tools

399 The highest values of tool temperature were observed in the case of the ZrN coated drill, and  
 400 the lowest in the case of the uncoated drill (Figures 18a-c). The increase in the temperature value for  
 401 a ZrN coated drill compared to a drill without a coating was about 20%. In the case of the TiAlN  
 402 coated drill, the value of cutting torque obtained ( $M_c$ ) is lower compared to the ZrN coated drill, but  
 403 it was still higher by approximately 13% in relation to the temperature value obtained with the use  
 404 of an uncoated drill.

405 In the case of the ZrN drill, the maximum temperature was 56.3°C. The smallest value of  
 406 temperature obtained in the drilling process relating to an uncoated drill was 38.5°C. This fact can be  
 407 explained by differentiation in both the coefficient of friction between the tool and the workpiece as  
 408 well as in the value of the thermal conductivity coefficient resulting from the type of tool coating. The  
 409 ZrN coating has a much lower heat transfer coefficient compared to the TiAlN coating (Table 2).  
 410 This causes the ZrN coating to be a barrier to removing heat from the cutting zone. In addition, the  
 411 MDF panel is characterised by a relatively low value of thermal conductivity.

412 The results of the statistical analysis (Table 8) allow us to reject, at a significance level  $p = 0.000$ ,  
 413 the hypothesis that the coating type and feed per revolution ( $f$ ) do not affect the temperature ( $T$ ). At  
 414 a significance level  $p = 0.006$  there is also a lack of influence of cutting speed ( $v_c$ ) on drill temperature.  
 415 There were no statistically significant interactions between the product factors analysed. A  
 416 correlation coefficient of the relation between the experimental and predicted values of tool  
 417 temperature is equal to approximately  $R^2 = 0.9184$  (Figure 18d).

418 **Table 8.** Significance level of the effect of cutting parameters on temperature ( $T$ ).

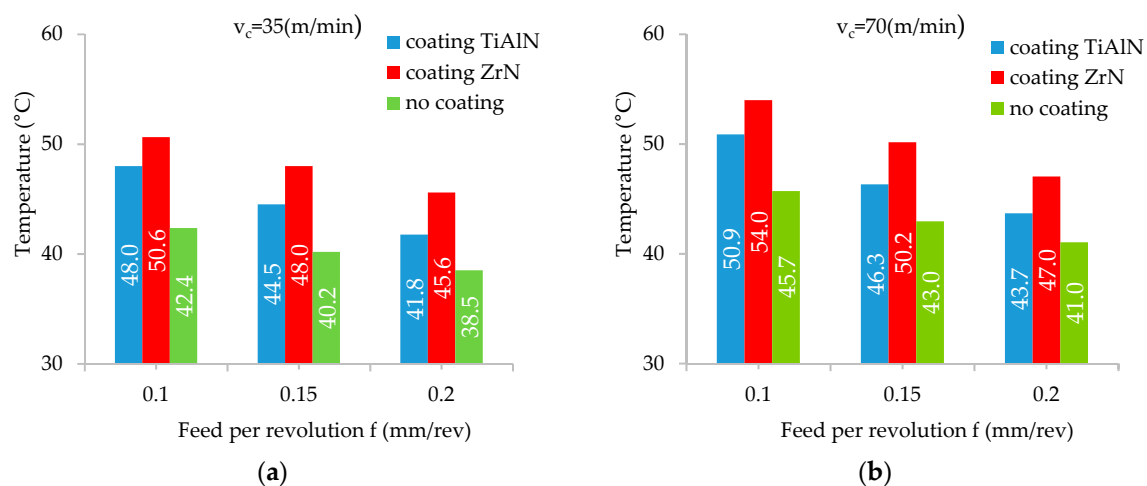
Tests Applied	Level of Significance ( $p \leq 0.05$ )
cutting speed ( $v_c$ )	0.006
feed per revolution ( $f$ )	0.000
coating	0.000
coating*cutting speed	0.998
coating*feed per revolution	0.943

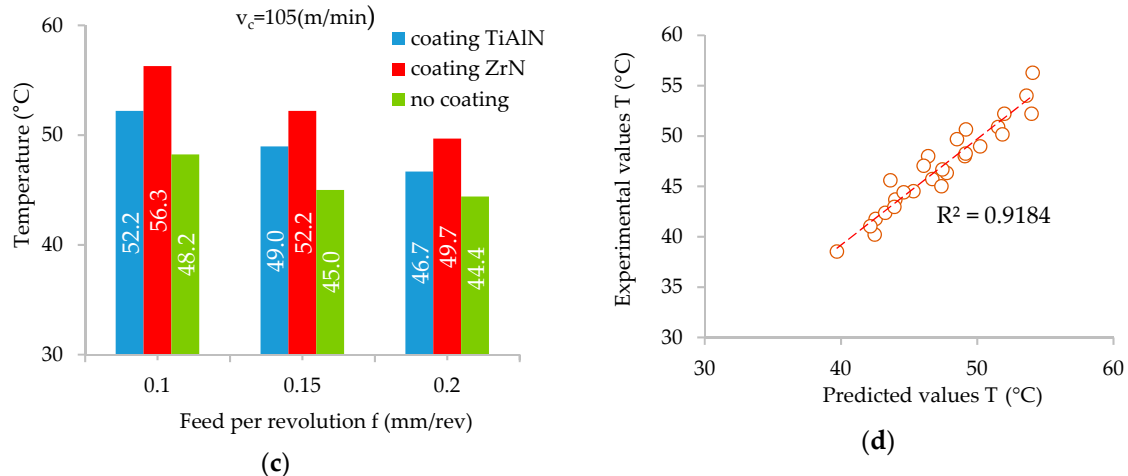
419 The temperature value of the cutting edge depending on the coating applied is expressed in the  
 420 form of the equations (7-9):

$$T \text{ (}^\circ\text{C)} = 53.791 - 62.601*f - 0.065*v_c, \text{ (ZrN)} \quad (7)$$

$$T \text{ (}^\circ\text{C)} = 55.978 - 65.241*f - 0.062*v_c, \text{ (TiAlN)} \quad (8)$$

$$T \text{ (}^\circ\text{C)} = 43.991 - 41.801*f - 0.078*v_c, \text{ (no coated)} \quad (9)$$





421 **Figure 18.** Influence of the feed value on the temperature value: (a) for a cutting speed of 35 m/min;  
 422 (b) for a cutting speed of 70 m/min; (c) for a cutting speed of 105 m/min; (d) correlation between the  
 423 experimental and predicted values of temperature.

#### 424 4. Conclusions

425 This paper presents the results of experimental investigations into the effect of coatings applied  
 426 to drill blades and cutting parameters on selected indices with regard to MDF machinability in the  
 427 drilling process. Based on the results obtained, it can be concluded that:

- 428 1. In the analysis of the values of thrust force ( $F_t$ ), cutting torque ( $M_c$ ) and surface roughness  
 429 parameter ( $R_a$ ) the layered structure of the MDF panel, which consists of layers of different  
 430 density and hardness, should be taken into account.
- 431 2. A significant effect of the type of drill coating on the value of all the MDF machinability indices  
 432 analysed was observed.
- 433 3. There is a dominant influence of both the feed per revolution ( $f$ ) and the type of tool coating  
 434 on thrust force ( $F_t$ ), cutting torque ( $M_c$ ) and cutting tool temperature in the MDF drilling  
 435 process.
- 436 4. The test results obtained show that the temperature in the drilling process increases with  
 437 increase in cutting speed ( $v_c$ ) but decreases with an increase of the feed per revolution ( $f$ ) value.  
 438 Temperature changes, depending on the coating type, vary on average by approximately 20%.
- 439 5. The feed per revolution ( $f$ ) and the type of drill coating had a significant influence on the value  
 440 of the roughness average ( $R_a$ ) parameter. It has been observed that in the outer layers of the  
 441 panel the ( $R_a$ ) parameter value has a lower value compared to that measured in the middle  
 442 layer.

443 In conclusion, the feed per revolution ( $f$ ) and the type of tool coating are the dominant  
 444 parameters that significantly affect the drilling process of the MDF board.

445 **Author Contributions:** K.S. and J.Z. designed and performed the experiments; K.S. and T.T. analysed the  
 446 experimental data obtained. Finally, K.S and T.T. contributed with resources (machine, tools, material, et al.) and  
 447 general supervision of the work.

448 **Acknowledgments:** The research has been carried out with the use of research equipment purchased under the  
 449 project "Establishment of the Intercollegiate Scientific and Research Laboratory in Stalowa Wola" under the  
 450 Operational Programme Development of Eastern Poland 2007-2013, Priority Axis I Modern Economy, Measure  
 451 1.3 Supporting Innovativeness pursuant to the contract No. POPW.01.03.00-18-016 / 12-00.

452 **Conflicts of Interest:** The authors declare no conflict of interest. The funders had no role in the design of the  
 453 study; in the collection, analyses, or interpretation of data; in the writing of the manuscript, or in the decision to  
 454 publish the results.

#### 455 References

- 456 1. Clarke, P.A. Panel products – past, present and future – developments 1991, *J. Inst. Wood Sci.* **1991**, *12*, 233–  
457 241.
- 458 2. Davim, J.P.; Clemente, V.C.; Silva S. Surface roughness aspects in milling MDF (medium density  
459 fibreboard). *Int. J. Adv. Manuf. Tech.* **2009**, *40*, 49-55. DOI: 10.1007/s00170-007-1318-z.
- 460 3. Davim, P.; Rubio C.; Abrao, M. Delamination assessment after drilling medium-density fibreboard (MDF)  
461 by digital image analysis. *Holzforschung* **2007**, *61*, 294-300. DOI: 10.1515/HF.2007.066.
- 462 4. Engin, S.; Altintas, Y.; Amara, F.B. Mechanics of routing medium density fibreboard. *Forest Prod. J.* **2000**,  
463 *50*, 65–69.
- 464 5. Szwajka, K.; Trzepiecinski, T. On the machinability of medium density fiberboard by drilling. *BioResources*  
465 **2018**, *13*, 8263-8278. DOI: 10.15376/biores.13.4.8263-8278
- 466 6. Penman, D., Olsson, O.J.; Bowman C.C. Automatic inspection of reconstituted wood panels for surface  
467 defects. *Proc. Soc. Photo-Optical Instr. Eng.* **1993**, *1823*, 284-293. DOI: 10.1117/12.132084.
- 468 7. Bhattacharyya, D.; Allen, M.N.; Mander, S. J. Cryogenic machining of Kevlar composites. *Mater. Manuf.*  
469 *Process* **1993**, *8*, 631-652. DOI: 10.1080/10426919308934871.
- 470 8. Costes, J.; Larricq, P. Towards high cutting speed in wood milling. *Ann. For. Sci.* **2002**, *59*, 857-865.
- 471 9. Dippon, J.; Ren, H.; Amara, F.B.; Altintas, Y. Orthogonal cutting mechanics of medium density fibreboards.  
472 *Forest Prod. J.* **2000**, *50*, 25–30.
- 473 10. Gordon, S.; Hillery, M.T. A review of the cutting of composite materials. *P. I. Mech. Eng. L-J. Mat.* **2003**, *217*,  
474 35-45. DOI: 10.1177/146442070321700105.
- 475 11. Nouari, M.; Makich, H. On the physics of machining titanium alloys: Interactions between cutting  
476 parameters, microstructure and tool wear. *Metals* **2014**, *4*, 335-358. DOI: 10.3390/met4030335.
- 477 12. Haddag, B. Metals machining - Recent advances in experimental and modeling of the cutting process.  
478 *Metals* **2018**, *8*, 1053. DOI: 10.3390/met8121053.
- 479 13. Wyeth, D.; Goli, G.; Atkins, A. Fracture toughness, chip types and the mechanics of cutting wood.  
480 *Holzforschung* **2009**, *63*, 168-180. DOI: 10.1515/HF.2009.017.
- 481 14. Marchal, R.; Mothe, F.; Denaud, L.; Thibaut, B.; Bleron L. Cutting forces in wood machining—Basics and  
482 applications in industrial processes. *Holzforschung* **2009**, *63*, 157-167. DOI: 10.1515/HF.2009.014.
- 483 15. Szwajka, K.; Trzepiecinski T. An examination of the tool life and surface quality during drilling melamine  
484 faced chipboard. *Wood Res.-Slovakia* **2017**, *62*, 307-318.
- 485 16. Djouadi, A.; Beer, P.; Marchal, R.; Sokolowska, A.; Lambertin, M.; Precht, W.; Nouveau C. Antiabrasive  
486 coatings: application for wood processing. *Surf. Coat. Tech.* **1999**, *116–119*, 508–516. DOI: 10.1016/S0257-  
487 8972(99)00236-4.
- 488 17. Djouadi, A.; Nouveau, C.; Beer, P.; Lambertin M. Cr<sub>x</sub>N<sub>y</sub> hard coatings deposited with PVD method on tools  
489 for wood machining. *Surf. Coat. Tech.* **2000**, *133-134*, 478-483. DOI: 10.1016/S0257-8972(00)00980-4.
- 490 18. Faga, M.G.; Settineri L. Innovative anti-wear coatings on cutting tools for wood machining. *Surf. Coat. Tech.*  
491 **2006**, *201*, 3002–3007. DOI: 10.1016/j.surfcoat.2006.06.013.
- 492 19. Nouveau, C.; Djouadi, A.; Marchal, R.; Lambertin M. Application of CrAlN coatings on carbide substrates  
493 in routing of MDF. *Wear* **2007**, *263*, 1291-1299. DOI: 10.1016/j.wear.2006.12.069.
- 494 20. Nouveau, C.; Jorand, E.; Deces-Petit, C.; Labidi, C.; Djouadi, A. Influence of carbide substrates on  
495 tribological properties of chromium and chromium nitride coatings: application to wood machining. *Wear*  
496 **2005**, *258*, 157–165. DOI: 10.1016/j.wear.2004.09.034.
- 497 21. Pinheiro, D.; Vieira, M.T.; Djouadi, A. Avantages of depositing multilayer coatings for cutting wood-based  
498 products. *Surf. Coat. Tech.* **2009**, *203*, 3197–3205. DOI: 10.1016/j.surfcoat.2009.03.052.
- 499 22. Szwajka, K.; Trzepiecinski, T. Effect of tool material on tool wear and delamination during machining of  
500 particleboard. *J. Wood Sci.* **2016**, *62*, 305-315. DOI: 10.1007/s10086-016-1555-6
- 501 23. Sedlecký, M. Surface roughness of medium-density fiberboard (MDF) and edge-glued panel (EGP) after  
502 edge milling. *BioResources* **2017**, *12*, 8119-8133. DOI: 10.15376/biores.12.4.8119-8133.
- 503 24. Tiryaki, S.; Hamzaçebi, C.; Malkoçoğlu, A. Evaluation of process parameters for lower surface roughness  
504 in wood machining by using Taguchi design methodology. *Eur. J. Wood Wood Prod.* **2015**, *73*, 537-545. DOI:  
505 10.1007/s00107-015-0917-x.
- 506 25. Boucher, J.; Méausoone, P.-J.; Martin, P.; Achet, S.; Perrin, L. Influence of helix angle and density variation  
507 on the cutting force in wood-based products machining. *J. Mater. Process. Tech.* **2007**, *189*, 211-218.
- 508 26. Gurau, L.; Mansfield-Williams, H.; Irle, M. Processing roughness of sanded wood surfaces. *Holz als Roh und*  
509 *Werkstoff* **2005**, *63*, 43-52. DOI: 10.1007/s00107-004-0524-8.

- 510 27. Thoma, H.; Peri, L.; Lato E. Evaluation of wood surface roughness depending on species characteristics..  
511 *Maderas: Ciencia y Tecnología* **2015**, *17*, 285-292. DOI: 10.4067/S0718-221X2015005000027.
- 512 28. Akgül, M.; Korkut, S.; Çamlıbel, O.; Candan, Z.; Akbulut T. Wettability and surface roughness  
513 characteristics of medium density fiberboard panels from rhododendron (*Rhododendron ponticum*)  
514 biomass. *Maderas: Ciencia y Tecnología* **2012**, *14*, 185-193. DOI: 10.4067/S0718-221X2012000200006.
- 515 29. Novák, V.; Rousek, M.; Kopecký Z. Assessment of wood surface quality obtained during high speed milling  
516 by use of non-contact method. *Drvena Industrija* **2011**, *62*, 103-115. DOI: 10.5552/drind.2011.1027.
- 517 30. Taylor, J.B., Carrano, A.L.; Lemaster, R.L. Quantification of process parameters in a wood sanding  
518 operation. *Forest Prod. J.* **1999**, *49*, 41-46.
- 519 31. Barčík, Š.; Gašparík, M. Effect of tool and milling parameters on the size distribution of splinters of planed  
520 native and thermally modified beech wood. *BioResources* **2014**, *9*, 1346-1360. DOI: 10.15376/biores.9.1.1346-  
521 1360.
- 522 32. Gaitonde, N.; Karnik, R.; Davim, P. Taguchi multiple-performance characteristics optimization in drilling  
523 of medium density fiberboard (MDF) to minimize delamination using utility concept. *J. Mater. Process. Tech.*  
524 **2008**, *196*, 73-78. DOI: 10.1016/j.jmatprotec.2007.05.003.
- 525 33. Škaljić, N.; Beljo-Lučić, R.; Čavlović, A.; Obućina, M. Effect of feed rate and wood species on roughness of  
526 machined surface. *Drvena Industrija* **2009**, *60*, 229-234. DOI: 10.1007/s10086-004-0655-x.
- 527 34. Szwajka, K.; Trzpiecinski, T. The influence of machining parameters and tool wear on the delamination  
528 process during milling of melamine-faced chipboard. *Drewno* **2017**, *60*, 117-131. DOI: 10.12841/wood.1644-  
529 3985.189.09.
- 530 35. Kvietková, M.; Gašparík, M.; Gaff, M. Effect of thermal treatment on surface quality of beech wood after  
531 plane milling. *BioResources* **2015**, *10*, 4226-4238. DOI: 10.15376/biores.10.3.4226-4238.
- 532 36. Lin, R.J.T.; van Houts, J.; Bhattacharyya, D. Machinability investigation of medium-density fibreboard.  
533 *Holzforschung* **2006**, *60*, 71-77. DOI: 10.1515/HF.2006.013.
- 534 37. Sütçü, A. Investigation of parameters affecting surface roughness in CNC routing operation on wooden  
535 EGP. *BioResources* **2013**, *8*, 795-805. DOI: 10.15376/biores.8.1.795-805.
- 536 38. Davim, J.P.; Reis, P.; Antonio C.C. Experimental study of drilling glass fiber reinforced plastics (GFRP)  
537 manufactured by hand lay-up. *Compos. Sci. Technol.* **2004**, *64*, 289-297.
- 538 39. Candan, Z.; Büyüksarı, U.; Korkut, S.; Unsal, O.; Çakıcıer, N. Wettability and surface roughness of  
539 thermally modified plywood panels. *Ind. Crop. Prod.* **2012**, *36*, 434-436. DOI: 10.1016/j.indcrop.2011.10.010.
- 540 40. Liu, D.; Tang, Y.; Cong, W. A review of mechanical drilling for composite laminates. *Compos. Struct.* **2012**,  
541 *94*, 1265-1279.